Spectroscopy and laser performance of Nd doped gadolinium lithium fluoride

Cite as: Journal of Applied Physics **74**, 790 (1993); https://doi.org/10.1063/1.354867
Submitted: 22 December 1992 . Accepted: 14 April 1993 . Published Online: 04 June 1998

X. X. Zhang, A. B. Villaverde, M. Bass, B. H. T. Chai, H. Weidner, R. I. Ramotar, and R. E. Peale

Spectroscopy and laser performance of Nd doped gadolinium lithium fluoride

X. X. Zhang, A. B. Villaverde,[a] M. Bass,[b] and B. H. T. Chai[c]
Center for Research in Electro-optics and Lasers (CREOL), University of Central Florida, Orlando, Florida 32826

H. Weidner, R. I. Ramotar, and R. E. Peale
Department of Physics, University of Central Florida, Orlando, Florida 32816

(Received 22 December 1992; accepted for publication 14 April 1993)

A comprehensive investigation on the spectroscopic properties and laser performance of Nd^{3+} doped $GdLiF_4$ (GLF), a new laser crystal, is reported. Our high resolution absorption and emission spectra for GLF are nearly identical to those of Nd:$LiYF_4$ (YLF), a well known laser crystal, strongly suggesting that the two crystals are isostructural. The laser performance of Nd:GLF is very similar to that of Nd:YLF. A maximum laser-pump-laser slope efficiency of 68% and 67% was obtained for low (1.0 at. %) and high (4.0 at. %) Nd concentration GLF respectively. Concentration quenching of the fluorescence decay time was observed and appears to be due to the dipole-dipole interaction between the isolated Nd^{3+} ions and Nd^{3+} ion pairs.

I. INTRODUCTION

Diode pumped, all solid state, Nd^{3+} lasers have received a great deal of attention recently because of their potential small size, high efficiency, and long operating lifetime. So far Nd:$LiYF_4$ (YLF) and Nd:$Y_3Al_5O_{12}$ (YAG) are the only commercially available crystals for such applications. Even though YAG and YLF are both good hosts, they can be doped with a maximum of only about 1 at. % Nd^{3+} without unacceptable degradation of crystal quality. This limitation on the Nd^{3+} concentration in YLF and YAG restricts some practical applications. We have recently demonstrated the efficient, low threshold laser performance of a new crystal—Nd^{3+}:$GdLiF_4$ (GLF),[1] which is capable of accommodating much higher Nd^{3+} concentration. So far crystals with a Nd^{3+} concentration four times as high as that in commercially available YLF and YAG crystals have been grown and demonstrated to lase efficiently. Preliminary studies[1] showed that the spectroscopic properties and lasing performance of GLF are very similar to those of YLF.

Nd:YLF oscillates, naturally polarized, at two wavelengths, 1.053 μm (σ polarization) and 1.047 μm (π polarization),[2] which match the gain curves of phosphate and fluorophosphate glass lasers.[3,4] Nd:YLF exhibits very weak thermal lensing,[5] which provides for a high ratio of TEM_{00} to multimode average power.[6] Nd:YLF also has about a factor of two longer fluorescence decay time than YAG,[7] a significant advantage for cw applications. Since the high resolution spectroscopic studies presented in this article confirm our earlier finding[1] that GLF is isostructural with YLF, Nd:GLF is expected to inherit most of the properties mentioned above from Nd:YLF. With its additional capability of accepting more Nd^{3+} ions, Nd:GLF may be attractive for many applications.

In this article, the energy levels of Nd^{3+} in GLF have been derived from high resolution, high frequency-accuracy transmission and emission spectra obtained by Fourier transform spectroscopy. Comparison is made with data for Nd:YLF. The concentration dependence of the fluorescence decay time of Nd^{3+} ions in GLF was investigated and the concentration quenching mechanism is discussed. The stimulated emission cross section of Nd:GLF is estimated by comparing its laser performance to that of Nd:YLF.

II. SPECTROSCOPIC PROPERTIES

Spectroscopy was performed on three samples grown by a modified Czochralski technique.[1] The Nd^{3+} doping concentrations in the melt were 1.3, 2.5, and 5.0 at. %, respectively. The actual Nd^{3+} concentrations in the grown crystals are estimated to be 1.0, 2.0, and 4.0 at. % since the distribution coefficient of Nd^{3+} in GLF is about 0.8.

In order to understand the gross spectroscopic characteristics of Nd:GLF we first present low resolution, room temperature absorption data. Low resolution absorption spectra were taken with a Perkin–Elmer 330 spectrophotometer. The resolution was about 1 nm. The room temperature polarized absorption spectra of 1.0 at. % Nd^{3+}:$GdLiF_4$ are given in Fig. 1. The absorption spectra are almost identical with those of Nd:YLF[7] except for the existence of the absorption features in the region from 250 to 320 nm in the Nd:GLF spectra originating from absorption by the Gd^{3+} ions ($^8S_{7/2}$ to $^6P_{3/2}$-$^6P_{7/2}$ and $^6I_{7/2}$-$^6I_{17/2}$)[8] of the host. The absorption features of 4.0 at. % Nd^{3+}:GLF are the same as those of 1.0 at. % Nd^{3+}:GLF, with the absorption coefficient almost four times as high as

[a]On leave from Universidade Estadual de Campinas, Campinas, SP, Brazil.
[b]Also with Departments of Physics and Electrical and Computer Engineering.
[c]Also with Departments of Physics and Mechanical Engineering.

 0021-8979/93/74(2)/790/7/$6.00

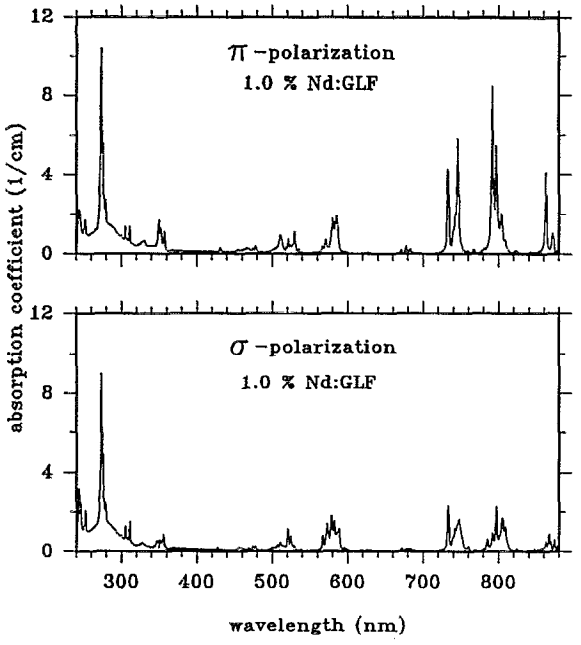

FIG. 1. Polarized absorption spectra of $Nd:GdLiF_4$ at room temperature.

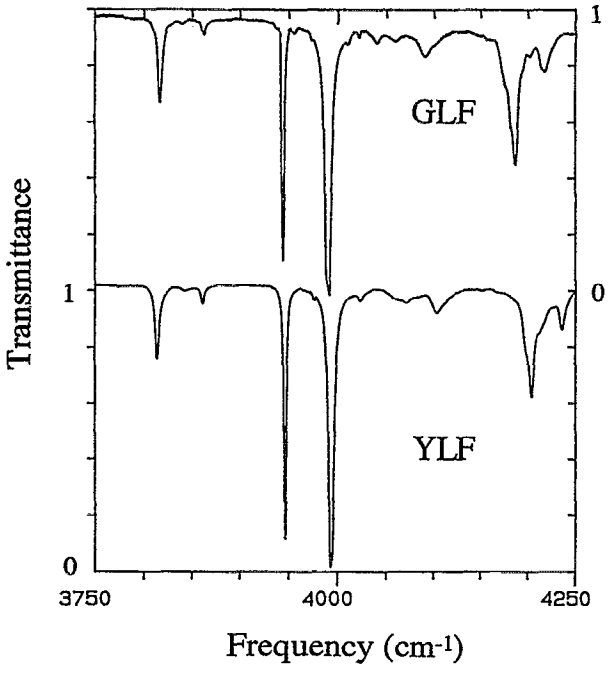

FIG. 3. Portion of π polarization high resolution transmission spectra of Nd:GLF and Nd:YLF ($^4I_{9/2} \rightarrow {}^4I_{13/2}$) at 80 K.

that of the latter. The absorption spectra in the diode pumping region (around 800 nm) for both concentrations are shown in Fig. 2.

In order to determine the energy level positions high resolution transmission and emission spectra were measured with a Bomem DA8 Fourier transform spectrometer at 80 and 300 K sample temperatures. The high frequency accuracy of the Fourier technique is well known, being ± 0.004 cm^{-1} at 2000 cm^{-1} for the Bomem. The resolution was chosen to be 1 cm^{-1} from 500 to 10 000 cm^{-1}, and 2 cm^{-1} at higher frequencies. Both transmission and emission spectra were measured in vacuum.

A portion of the π-polarized 80 K transmission spectra ($^4I_{9/2} \rightarrow {}^4I_{13/2}$) of Nd:GLF is given in Fig. 3 along with that of Nd:YLF for comparison. The extremely close similarity of the spectra in the two materials is apparent: the number of lines, their frequency positions, their relative strengths, and their widths are nearly identical. The polarization dependences are also the same in each.

Photoluminescence was excited with a cw multiline Argon ion laser and was detected with a Si photodiode. The polarized emission spectra in the 1 μm region of 1.0 at. % Nd:GLF are shown in Fig. 4(a) for 80 K and Fig. 4(b) for 300 K. The main peak is centered at 1.047 μm for π polarization ($E \| C$) and at 1.053 μm for σ polarization ($E \perp C$) at 300 K. The structures of the emission spectra for 4.0 at. % Nd:GLF are almost identical to those of 1.0 at. % Nd:GLF. They are again nearly identical to those of Nd:YLF, also measured by us. The spectral widths in GLF are somewhat broader than those in YLF. The full widths at half maximum (FWHM) for both 1.047 and 1.053 μm lines are given in Table I for Nd:GLF and Nd:YLF. The widths in GLF are independent of Nd concentration within experimental error.

The energy levels of Nd^{3+}:GLF and Nd^{3+}:YLF were

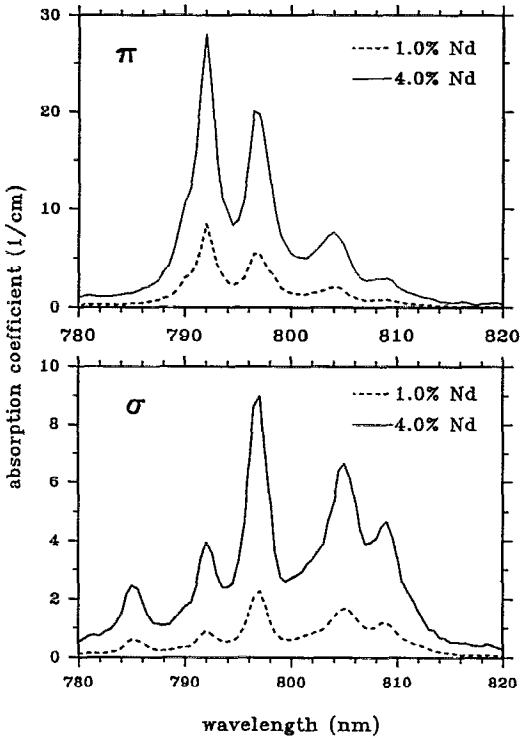

FIG. 2. Polarized absorption spectra of $Nd:GdLiF_4$ in the 800 nm region at room temperature.

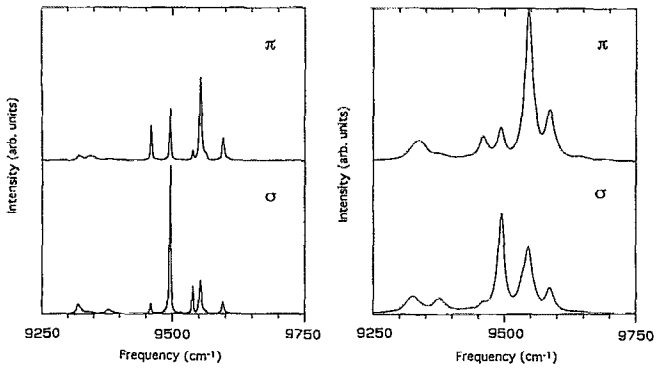

FIG. 4. Polarized emission spectra of 1.0 at. % Nd:$GdLiF_4$ in the 1 μm region at 80 K (a) and 300 K (b)

derived from the high resolution transmission and emission spectra at 80 K and are given in Table II. Although the energy levels of Nd^{3+}:YLF have been reported,[7,9,10] our accurate YLF values differ by more than the line widths from values previously obtained using conventional grating techniques.[10]

The fluorescence decay measurements employed a flash-lamp-pumped, Q-switched Cr:LiSAF laser (pulse width=80 ns, wavelength=797 nm) as the excitation source. The signal was detected through a 1/4 m monochromator with an S-1 photomultiplier and a Tektronix 2440, 300 MHz, digital oscilloscope. The decay curves of the $^4F_{3/2}$ level fluorescence of Nd^{3+} in GLF with different Nd^{3+} concentrations at room temperature are given in Fig. 5. The decay curves are nonexponential for all the samples studied at room temperature. Hence, we discuss the dynamics in terms of an "effective decay time," defined by[11]

$$\tau_{\text{eff}}=1/I_0\int_0^\infty I(t)dt, \tag{1}$$

where I_0 is the initial luminescence intensity and $I(t)$ is the decay curve. This effective decay time is slightly larger than the $1/e$ decay time in our measurements, since the observed nonexponential decay consists of a faster decay at

TABLE I. Full widths at half maximum (cm^{-1}) of the main emission peaks in Nd:GLF and Nd:YLF at 80 and 300 K.

	80 K		300 K	
Crystals	1.047 μm π polarization	1.053 μm σ polarization	1.047 μm π polarization	1.053 μm σ polarization
1.0 at.% Nd:GLF	4.6	3.0	18.0	15.4
4.0 at.% Nd:GLF	5.0	3.5	17.3	15.3
1.2 at.% Nd:YLF	2.9	2.2	12.4	11.1

TABLE II. Energy levels (cm^{-1}) of Nd^{3+} in GLF and YLF.

Spectral term	GLF	YLF
$^4I_{9/2}$	0	0
	128.0	132.1
	182.0	182.5
	239.0	247.2
	496.0	526.6
$^4I_{11/2}$	1992.7	1997.1
	2036.4	2040.1
	...	2042.4
	2071.8	2077.0
	2211.4	2226.8
	2247.0	2261.9
$^4I_{13/2}$	3944.3	3947.2
	3973.7	3975.9
	3990.3	3993.9
	4021.9	4023.5
	4186.6	4204.4
	4202.6	4214.3
	4221.8	4239.5
$^4I_{15/2}$	5855.5	5848.5
	5911.0	5909.5
	5949.7	5944.9
	6025.2	6031.5
	6295.2	6312.0
	6326.7	6346.1
	6366.0	6390.0
	6401.4	6431.8
$^4F_{3/2}$	11530.9	11535.7
	11588.7	11594.5
$^4F_{5/2}$, $^2H_{9/2}$	12534.7	12535.3
	12546.4	12544.9
	12617.9	12625.7
	12641.0	12641.8
	12656.1	12663.0
	12727.6	12729.5
	12792.7	12803.7
	12823.7	12829.4
$^4F_{7/2}$, $^4S_{3/2}$	...	13408.4
	13493.9	13494.5
	13516.0	13518.7
	13625.8	13637.1
	13638.1	13645.3
	13647.8	13656.1
$^4F_{9/2}$	14742.8	14745.7
	14769.1	14774.0
	14868.8	14873.8
	14882.9	14887.3
$^2H_{11/2}$	15961.1	15962.9
	15990.9	15989.8
	16046.4	16050.4
	...	16122.1
	16125.9	16133.9
$^4G_{5/2}$, $^2G_{7/2}$	17154.0	17152.6
	17261.0	17261.6
	17292.3	17288.3
	17404.9	17400.4
	17393.5	17408.9
	17461.1	17466.3
	17626.6	17640.4
$^4G_{7/2}$	19060.0	19055.8
	19068.0	19067.0
	19166.0	19169.0
	19203.1	19199.1

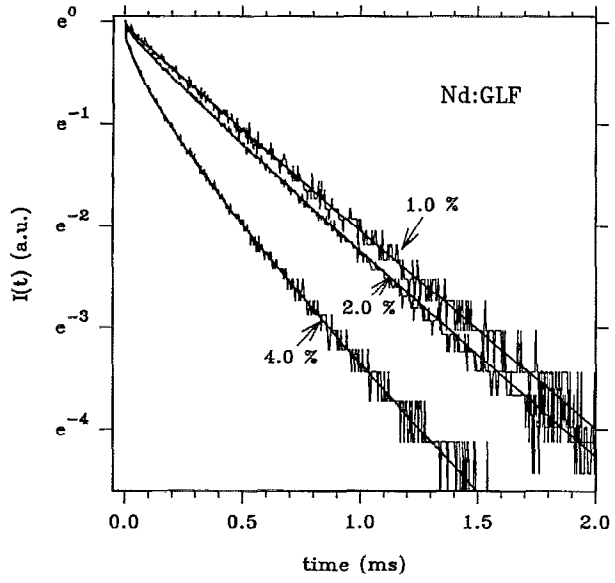

FIG. 5. Decay of the $^4F_{3/2}$ level fluorescence of Nd^{3+}:$GdLiF_4$ at room temperature. Solid lines are the calculated results using Eq. (2).

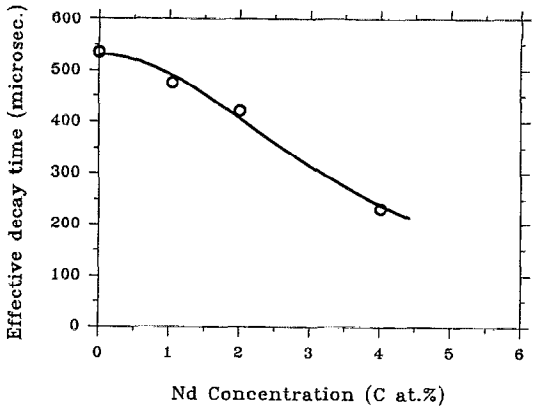

FIG. 6. Room temperature effective decay time of Nd^{3+}:$GdLiF_4$ as a function of Nd^{3+} concentration. The solid line is the calculated result using Eq. (4).

early times and a slower one at later times. Table III gives the effective and the $1/e$ decay times for samples with different Nd concentrations. The extrapolated zero concentration values will be discussed below. The effective decay time at room temperature is plotted as a function of Nd concentration in Fig. 6.

III. LASER PERFORMANCE

For laser experiments two GLF samples (with Nd^{3+} concentration of 1.0 and 4.0 at. %) were cut with flat and parallel faces containing the c axis. They were antireflection (AR) coated from 1.0 to 1.1 μm. The crystal lengths, 6 mm for the 1.0 at. % Nd crystal and 1.8 mm for the 4.0 at. % Nd crystal, were chosen so that the pump light absorbed would be about the same in each. The laser test employed a concave (5 cm radius) reflector (high reflectivity @ 1.0–1.1 μm and high transmission @ 790–810 nm) and a flat partial reflector (partial reflectivity @ 1.0–1.1 μm and high transmission @ 790–810 nm) to form the laser cavity. Different partial reflectors with reflectivities of 98.8%, 97.0%, and 95.0% were used to test the laser performance. Both pulsed and cw laser pumped operation were studied. Pulsed excitation was achieved with a long pulse Cr:LiSAF laser. cw excitation employed a Ti:sapphire laser. Both lasers were tuned to 797 nm to match one of the absorption peaks of the Nd^{3+} ion in GLF. The spectral bandwidth of the Cr:LiSAF laser was about 4 nm, whereas that of the Ti:sapphire was less than 1 nm. The pump light was focused into the 4.5-cm-long laser cavity with a 10 cm focal length lens, and the crystal tested was placed about 4 mm in front of the flat mirror (output coupler). For comparison, a commercial 1.2% Nd:YLF crystal from Lightning Optics, Inc. (3 mm in diameter×6 mm in length, and AR coated) was tested in the same resonator using the same pumping conditions.

Lasing from Nd:GLF is linearly polarized along the c axis (π polarization) and occurs at 1.047 μm, the same wavelength as that of Nd:YLF. The observed maximum slope efficiencies for the two GLF crystals are compared with those for the YLF crystal in Table IV for both types of operation. The cw absorbed power thresholds in Nd:GLF and Nd:YLF for different output couplers are given in Table V. For 4.0 at. % Nd:GLF, the variation of the slope efficiency in cw operation with the transmission of the output coupler is shown in Table VI.

TABLE III. Effective and $1/e$ decay times and the γ parameter of Nd^{3+} in GLF with different Nd^{3+} concentrations. The zero concentration values have been extrapolated from theoretical decay curves (see Sec. IV).

Nd concentration (at.%)	Effective decay time (μs)	$1/e$ decay time (μs)	γ ($ms^{-1/2}$)
0	535	535	0
1.0	475	468	0.174
2.0	421	404	0.371
4.0	231	192	1.473

IV. DISCUSSION

The near identity of the high resolution, low temperature transmission spectra (Fig. 3) of Nd^{3+} in GLF and YLF indicates that each host has the same (S_4^{12}) site symmetry with nearly identical crystal-field parameters. This strongly suggests that GLF and YLF are isostructural (space group $C_{4h}^{6}{}^{12}$). It can be seen from Table II that the

TABLE IV. Observed laser-pump-laser maximum slope efficiencies (%) for Nd:GLF and Nd:YLF.

Pulsed			cw		
1.2 at.% Nd:YLF	1.0 at.% Nd:GLF	4.0 at.% Nd:GLF	1.2 at.% Nd:YLF	1.0 at.% Nd:GLF	4.0 at.% Nd:GLF
70	62	67	70	68	57

TABLE V. Absorbed power (mW) thresholds as a function of the output coupler transmission (T) for different crystals.

	Thresholds		
T (%)	1.2 at.% Nd:YLF	1.0 at.% Nd:GLF	4.0 at.% Nd:GLF
1.2	5.5	7.1	10.9
3.0	8.8	9.7	18.4
5.0	11.5	14.1	20.9

total crystal field splitting of each Nd^{3+} term in GLF is slightly smaller than in YLF. The center of gravity of each spectral term is slightly lower in GLF than in YLF except for the $^4G_{7/2}$ term. These results indicate that the crystal field is slightly weaker in GLF.

The apparent independence of the emission width on Nd concentration in GLF (Table I) suggests that pairing may be negligible even at such high concentrations as 4%. However, our detailed dynamical studies indicate otherwise. As shown in Fig. 5, all the decay curves for all the Nd:GLF samples studied are nonexponential. The most likely physical processes that can account for such behavior is energy transfer from excited Nd^{3+} ions (donors) to some energy accepting centers (acceptors). In the following few paragraphs we will show that energy transfer can indeed account for the non-exponential characteristics of the fluorescence decays and that Nd^{3+}-Nd^{3+} ion pairs can be considered as the energy accepting centers.

Under the assumption of a dipole-dipole interaction between the donors and acceptors, the decay of the donor emission can be described by the formula:[13]

$$I(t)=I_0\exp(-t/\tau_D-\gamma t^{1/2}), \tag{2}$$

where τ_D is the decay time of donors in the absence of the acceptors and γ takes the form:

$$\gamma=4/3\pi^{3/2}n_A\sqrt{C_{\mathrm{DA}}}, \tag{3}$$

where n_A is the acceptor concentration and C_{DA} is a measure of the donor-acceptor coupling strength. All the decay curves in Fig. 5 can be well described by Eq. (2), as seen from the figure, indicating that the interaction which is responsible for the energy transfer is dipole-dipole coupling (other multi-pole interaction mechanisms were also unsuccessfully tried to fit the decays). All these decay curves are fit to data by using the same τ_D parameter, 535 μs. Since τ_D is the decay time in the absence of energy transfer, τ_D can be regarded as the decay time when the Nd concentration approaches zero. It is therefore included in Table III as the fluorescent lifetime at very low Nd^{3+} concentrations.

TABLE VI. Variation of slope efficiency with the output coupler transmission (T) for 4.0 at.% Nd:GLF in cw operation.

T (%)	Slope efficiency (%)
1.2	41
3.0	55
5.0	57

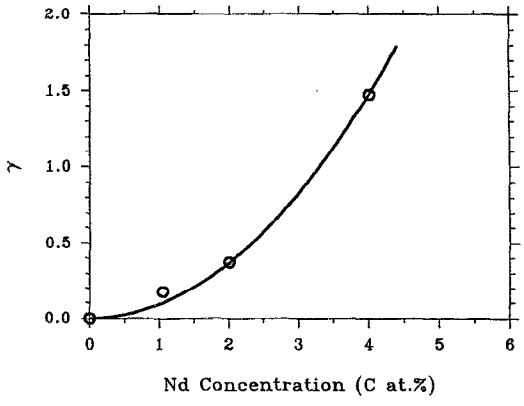

FIG. 7. Energy transfer parameter γ as a function of Nd concentration in GLF. The solid line shows that γ increases quadratically with Nd concentration.

Concentration quenching is demonstrated in Fig. 6, in which the effective decay time of the $^4F_{3/2}$ level is plotted as a function of Nd concentration in GLF. The dependence of the effective decay time on the Nd concentration can be described, as shown by the solid line in the figure, by the following relation:

$$\tau=\tau_0/[1+(C/C_0)^2], \tag{4}$$

where τ_0 is the intrinsic decay time without the presence of concentration quenching, C is the Nd concentration, and C_0 is the Nd concentration at which the decay time decreases to half of the intrinsic decay time. This is consistent with the above conclusion that the concentration quenching mechanism is dipole-dipole interaction.[14] The parameters used to calculate the curve in Fig. 6 were $\tau_0=530$ μs and $C_0=3.6$ at. %. τ_0 and τ_D are the same, within the experimental error, as expected.

The γ parameters used in the decay curve calculations are also listed in Table III for different samples and plotted as a function of Nd concentration in Fig. 7 which shows that γ increases quadratically with increasing Nd concentration. It can be seen from Eq. (3) that γ is directly proportional to n_A, the acceptor concentration, since C_{DA} is a measure of the donor-acceptor coupling strength and should not be concentration dependent. Therefore Fig. 7 indicates that n_A increases quadratically with the Nd concentration. This is very suggestive that the "acceptors" which are responsible for the nonexponential decay (energy transfer) are Nd^{3+}-Nd^{3+} ion pairs, since the concentration of the pairs should increase quadratically with the single ion concentration. This offers a very sensible mechanism for concentration quenching at least in Nd:GLF (i.e., the energy transfer from the single Nd^{3+} ions to the Nd^{3+}-Nd^{3+} ion pairs) without postulating the existence of the unknown "nonradiative" centers.[14] In the past, nonradiative centers were postulated[14] because spectroscopic ev-

idence for pairs was absent. However, the existence of the Nd^{3+}-Nd^{3+} pairs in YLF has been convincingly demonstrated spectroscopically.[15]

It can be seen from Table IV that the maximum slope efficiency of 1.0 at. % Nd:GLF (68%) is very close to that of YLF (70%). Considering the quantum defect resulting from the difference between the pump wavelength (797 nm) and the lasing wavelength (1.047 μm), one expects a maximum intrinsic slope efficiency of 76%. Therefore the observed slope efficiency is remarkable. However, the thresholds are slightly higher for GLF than YLF, as shown in Table V. We believe that this is due to higher loss in GLF, since we could see some visual scattering centers in the crystal and we could get a higher slope efficiency and a lower threshold by carefully positioning the sample in the cavity. The existence of inhomogeneities in the crystal is evidenced by the discrepancy between the slope efficiencies observed in pulsed and cw operation (the crystal position inside the cavity was not exactly the same for both operation).

The absorbed power threshold can be expressed as follows:[16]

$$P_{\text{th}}=\frac{\pi h\nu_p \delta}{4\sigma_e \eta_p \tau}(w_0^2+w_p^2), \tag{5}$$

where $h\nu_p$ is the pump photon energy, η_p is the pump quantum efficiency, τ is the upper level decay time, σ_e is the stimulated emission cross section, δ is the round-trip loss which includes both internal and external losses, and w_0 and w_p are the beam radii of the laser cavity mode and the pump beam respectively. $h\nu_p$, w_0, and w_p are the same for 1.2 at. % Nd:YLF and 1.0 at. % Nd:GLF. Assuming that δ and η_p are also the same for both crystals, one can estimate the stimulated emission cross section of 1.0 at. % Nd:GLF from the threshold data listed in Table V and the decay times of YLF (442 μs) and 1.0 at. % Nd:GLF (475 μs). The resulting estimated ratio between the stimulated emission cross sections of GLF and YLF varies from 0.72 to 0.84 depending on the transmission of the output coupler. This implies that the losses are not the same for both crystals. The actual cross section ratio should be larger than 0.72 since we expect that the loss is larger in GLF than in YLF. We expect the cross section of GLF to be very close to that of YLF (1.96×10^{-19} cm^2 at 1.047 μm for π polarization[11]).

It is more interesting to focus on the laser performance of the highly doped Nd:GLF (4.0 at. %) since the importance of GLF is its potential for high doping. Information on the intrinsic slope efficiency and passive loss in the crystal can be derived from the variation of measured slope efficiency with the output coupler transmission through the following simple relation[17]

$$\eta=\eta_0 T/(T+L), \tag{6}$$

where η is the measured slope efficiency, η_0 is the intrinsic slope efficiency, T is the transmission of the output coupler, and L is the double-pass passive loss. Equation (6) can be rewritten as

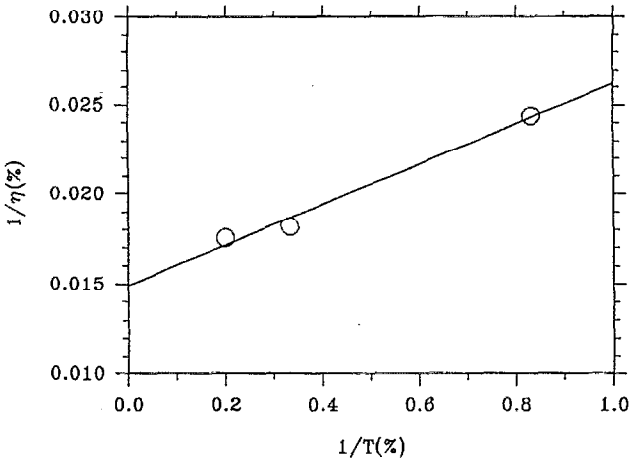

FIG. 8. Slope efficiency as a function of the transmission of the output coupler. The solid line is the calculated result using Eq. (7).

$$1/\eta=(L/\eta_0)(1/T)+1/\eta_0. \tag{7}$$

A plot of $1/\eta$ vs $1/T$ will give a straight line with a slope of L/η_0 and an intercept of $1/\eta_0$. Data given in Table VI are plotted in the form of Eq. (7) and shown in Fig. 8. The intrinsic slope efficiency η_0 and the double pass loss L derived from Fig. 8 are 67% and 0.75%, respectively for 4.0 at. % Nd:GLF. A similar study for 1.2 at. % Nd:YLF gives an intrinsic slope efficiency of 76% and a double pass loss of 0.45%. This again shows the higher loss in GLF. However, a slope efficiency of 67% for 4.0 at. % Nd:GLF is quite good considering that concentration quenching exists in this highly doped material. A 67% slope efficiency has been obtained in pulsed operation for 4.0 at. % Nd:GLF. Therefore it is reasonable to believe that the cw performance is limited only by the crystal quality. Further improvement of crystal quality is expected.

Using the measured thresholds, the losses calculated above, and the decay time data, the stimulated emission cross section of the high concentration Nd:GLF can be estimated using Eq. (5) assuming the experimental parameters are the same for both 4.0 at. % Nd:GLF and 1.2 at. % Nd:YLF. The resulting estimated ratio between the cross sections of Nd:GLF and Nd:YLF varies between 1.04 and 1.14 depending on the transmission of the output coupler. Taking into account the actual sizes of the pump beam and the laser mode in the cavity, which are larger for YLF since a longer crystal was used, the ratio should be slightly smaller than that obtained above.

V. CONCLUSIONS

Detailed high resolution transmission and emission spectra indicate that Nd^{3+} ions occupy sites of the same symmetry and nearly identical crystal field parameters in both YLF and the new crystal GLF. These results strongly suggest that GLF is isostructural to YLF. Energy levels of Nd^{3+}:GLF, reported here for the first time, show that the crystal field is slightly weaker in GLF than in YLF. The emission linewidth in Nd:GLF is slightly broader than in

YLF, being 18 cm^{-1} for the former and 12.4 cm^{-1} for the latter for the 1.047 μm line (π polarization). This may be useful in producing shorter pulses[18] since the length of the mode-locked pulses is approximately the inverse of the gain line width.[19] The intrinsic radiative decay time of Nd:GLF is 530 ± 5 μs, about the same as that of Nd:YLF.[11] Concentration quenching in this material is well explained by the energy transfer between single Nd^{3+} ions and Nd^{3+}-Nd^{3+} ion pairs via a dipole-dipole interaction mechanism. The stimulated emission cross section of Nd:GLF was estimated to be about the same as that for Nd:YLF. A 68% slope efficiency was measured for the low concentration Nd:GLF in cw operation and a 67% slope efficiency was projected for highly doped Nd:GLF in cw operation. The observed lower slope efficiency for highly doped Nd:GLF in cw operation is only limited by the crystal quality, which we are working to improve. Overall Nd:GLF is expected to be an effective laser material in a variety of applications, particularly in compact diode-pumped laser systems.

ACKNOWLEDGMENTS

This work was supported by the Defense Advanced Research Projects Agency (DARPA) and by the Florida High Technology and Industry Council. The authors would like to thank Dr. P. LiKamWa and Dr. A. Miller for the use of their Ti:sapphire laser and Lightning Optical Co. for providing the Nd:YLF crystal used in the laser comparison study. One of the authors (A. B. V.) also would like to acknowledge the financial support from CNPq-Conselho Nacional de Desenvolvimento Cientifico e Tecnologico do Brazil. R. E. P. acknowledges generous startup funding from the Division of Sponsored Research at the University of Central Florida.

[1] X. X. Zhang, M. Bass, A. B. Villaverde, J. Lefaucheur, A. Pham, and B. H. T. Chai, Appl. Phys. Lett. **62**, 1197 (1993).
[2] A. L. Harmer, A. Linz, D. Gabbe, L. Gillespie, G. M. Janney, and E. Sharpe, Bull. Am. Phys. Soc. **12**, 1068 (1967).
[3] J. Zimmerman, W. Knox, and W. Seka, Topical Meeting on Inertial Confinement Fusion, San Diego, CA, Feb., 1978, paper TUB 9-1.
[4] S. E. Stokowski, M. J. Weber, R. A. Saroyan, G. J. Linford, J. Wenzel, D. Blackburn, C. Brecher, and L. A. Riseberg, Topical Meeting on Inertial Confinement Fusion, San Diego, CA, Feb., 1978, paper TUB 12-1-4.
[5] J. E. Murray, IEEE J. Quantum Electron. **QE-19**, 488 (1983).
[6] T. M. Pollak, W. F. Wing, R. J. Grasso, E. P. Chicklis, and H. P. Jenssen, IEEE J. Quantum Electron. **QE-18**, 159 (1982).
[7] A. L. Harmer, A. Linz, and D. R. Gabbe, J. Phys. Chem. Sol. **30**, 1483 (1969).
[8] G. H. Dieke, *Spectra and Energy Levels of Rare Earth Ions in Crystals*, edited by H. M. Crosswhite and H. Crosswhite (Interscience, New York, 1968), p. 249.
[9] D. E. Wortman, J. Phys. Chem. Sol. **33**, 311 (1972).
[10] A. A. S. da Gama, G. F. de Sá, P. Porcher, and P. Caro, J. Chem. Phys. **75**, 2583 (1981).
[11] J. R. Ryan and R. Beach, J. Opt. Soc. Am. B **9**, 1883 (1992).
[12] P. Blanchfield, Tu Hailing, A. J. Miller, G. A. Saunders, and B. Chapman, J. Phys. C **20**, 3851 (1983).
[13] Th. Förster, Z. Naturforsch. **4a**, 321 (1949).
[14] D. L. Dexter and J. H. Schulman, J. Chem. Phys. **22**, 1063 (1954).
[15] R. B. Barthem, R. Buisson, J. C. Vial, and H. Harmand, J. Lumin. **34**, 295 (1986).
[16] T. Y. Fan and R. L. Byer, IEEE J. Quantum Electron. **QE-24**, 895 (1988).
[17] J. A. Caird, S. A. Payne, P. R. Staver, A. J. Ramponi, L. L. Chase, and W. F. Krupke, IEEE J. Quantum Electron. **QE-24**, 1077 (1988).
[18] P. Bado, M. Bouvier, and J. S. Coe, Opt. Lett. **12**, 319 (1987).
[19] A. Yariv, *Quantum Electronics*, 3rd ed. (Wiley, New York, 1989), p. 545.